Supporting Information for

Integrated Triplex LFIA Platform for Decentralized Molecular Subtyping of Breast Cancer

Wenting Gao[1], Iftak Hussain[2], Theopisti A. Nikolaou[1], Samantha Symons[1], Ganga Dripaul[1], Monalisa Almeida[1], Catherine Guo[2], Sally Adebamowo[3], Clement Adebamowo[3], and David Erickson[1,2]**

[1]*Meinig School of Biomedical Engineering, Cornell University, Ithaca, NY, USA*

[2]*Sibley School of Mechanical and Aerospace Engineering, Cornell University, Ithaca, NY, USA*

[2]*Greenebaum Comprehensive Cancer Center, and the Department of Epidemiology & Public Health, University of Maryland School of Medicine, Baltimore, MD, USA*

*Joint corresponding authors: David Erickson (de54@cornell.edu), and Clement Adebamowo (cadebamowo@som.umaryland.edu)

This PDF file includes:

SI Materials and Methods

Figures S1 to S7

Tables S1 to S5

Supporting Information (SI) Materials and Methods

Fluorometric LFIA Dipsticks Assembly and Preparation

LFIA dipsticks were fabricated using Whatman FF170HP membrane cards (Cytiva) with pre-adhered adhesive backing and CF5 absorbent pads (Cytiva). The nitrocellulose membrane integrated within the membrane cards had an average capillary flow rate of 45 s/cm, selected to enhance analyte-reagent interaction and improve detection sensitivity. Biorecognition elements (e.g. capture antibodies) were immobilized onto the nitrocellulose membrane using a Kinematic Automated Matrix 1600 dispenser at a precisely controlled dispensing rate of 1 μL/sec. Membranes were dried at 37°C for 2 hours under controlled humidity conditions before integration into the test strip to ensure long-term stability. Absorbent pads were assembled onto the polystyrene adhesive backing, maintaining a 2 mm overlap with the nitrocellulose membrane to facilitate efficient solution transfer.

Assembled LFIA dipsticks were dipped into 96-well plates containing 64 μL of sample mix/standard solutions and incubated for 20 min. Fluorescence signals were captured using a Nikon Eclipse TE2000-E inverted fluorescence microscope with the following scan parameters: excitation, 365 nm; emission, 610 nm; objective, 20× (NA 0.75); exposure time, 1000 ms; gain, 2×; binning, 1×1; filter cube, Ex 360–380 nm / DM 400 nm / Em 600–630 nm; image format, 16-bit TIFF. Images were converted to 8-bit greyscale using Fiji (ImageJ), and mean grey values of the test dot/line were calculated by averaging greyscale intensities.

Optimization of LFIA Parameters

Europium–streptavidin (Eu-SA) nanoparticles (Abcam, ab270228, 0.5% solids suspension) were used as the fluorescent reporters for all LFIA optimization experiments. Detection antibodies, capture antibodies, and recombinant protein standards for PR, ER, and HER2 were obtained from the R&D Systems DuoSet ELISA kits (PR: DYC5415; ER: DYC5715; HER2/ErbB2: DYC1129), ensuring consistency across reagents and standards. Control-line antibodies consisted of donkey anti-goat and donkey anti-sheep IgG (Bio-Techne, BAF109 and BAF016). The conjugation buffer was prepared in-house using 1xPBS supplemented with 5% sucrose, 1% BSA, and 0.5% Tween 20, and the running buffer was prepared using 1× PBS supplemented with 1× TBS, 1% (w/v) BSA, 1% (v/v) Tween-20, and 3% (w/v) sucrose.

To determine the optimal Eu-SA concentration, LFIA strips were prepared with Eu-SA conjugates at varying concentrations (0.001–0.01% solids). The conjugates were diluted in the conjugation buffer and optimized to maintain colloidal stability and prevent nanoparticle aggregation. Biotinylated bovine serum albumin (BSA) (Vector Laboratories, B-2007-10) was immobilized at the capture site, and fluorescence intensities were measured. The optimal Eu-SA concentration was determined based on the highest signal intensity with minimal background, with 0.005% solids providing the best performance.

Recombinant protein standards were diluted in 1× PBS supplemented with 1% BSA to stabilize protein structure and minimize nonspecific interactions during incubation. To optimize the concentration of biotinylated detection antibodies, LFIA strips were prepared with 0.005% Eu-

SA and tested with biotinylated antibodies at concentrations ranging from 0.005 mg/mL to 0.05 mg/mL for each biomarker. Fluorescence intensity increased with antibody concentration but plateaued beyond 0.01 mg/mL for HER2 and 0.024 mg/mL for PR and ER, where background noise also increased. These concentrations were selected as they provided optimal signal-to-noise ratios.

To determine the optimal control line antibody concentration, LFIA strips were prepared with a 1:1 mixture of donkey anti-goat and donkey anti-sheep IgG antibodies at concentrations ranging from 0.01 mg/mL to 0.25 mg/mL. The optimal concentration was identified as 0.1 mg/mL, as it provided consistent signal intensity at the control line while preventing excessive background fluorescence.

To optimize capture antibody concentrations, LFIA strips were prepared with varying antibody concentrations for each biomarker: 0.05 mg/mL, 0.1 mg/mL, and 0.5 mg/mL for PR; 0.05 mg/mL, 0.1 mg/mL, and 0.18 mg/mL for ER; and 0.1 mg/mL, 0.36 mg/mL, and 0.72 mg/mL for HER2. Test lines were spaced 3 mm apart, and each antibody was deposited at a final concentration of 0.1 mg/mL in 1× PBS supplemented with 2% sucrose to maintain bioactivity and prevent desiccation-related conformational changes. LFIA strips were incubated with spiked biomarker solutions (0–1000 pM), and fluorescence intensities of test lines were quantified using the PROVIDS reader system and the mean test-to-control (T/C) ratio was calculated. The optimal capture antibody concentrations were determined based on dose-response curves and signal stability, with 0.1 mg/mL for PR and ER, and 0.36 mg/mL for HER2 providing the highest test line intensity while avoiding steric hindrance effects.

Singleplex Quantitative LFIA of Human PR, ER, or HER2 Proteins

For full-strip singleplex LFIA targeting human total PR, ER, or HER2 proteins, conjugate pads were impregnated with Eu-SA conjugated biotinylated detection antibodies at optimized concentrations (0.024 mg/mL for PR and ER, and 0.01 mg/mL for HER2) in the previously described conjugation buffer. Incubation pads were prepared by pre-treatment with Candor Blocking Solution (Candor, 100050), followed by sequential washing with PBST (0.05% Tween-20 in 1× PBS). Both conjugate and incubation pads were air-dried at 37°C for at least 30min and stored desiccated until assembly.

Singleplex LFIA strips were sequentially assembled by affixing the sample pad, conjugate pad, incubation pad, and absorbent pad onto pre-adhesive nitrocellulose backing cards. Each component overlapped by 2 mm to ensure regulated fluid flow and optimal antigen-antibody interactions (Supplementary Fig. 2b). Assembled strips were then cut into consistent 4 mm widths. The Nitrocellulose membranes contained immobilized capture antibodies at concentrations of 0.1 mg/mL for PR and ER and 0.36 mg/mL for HER2. A control line consisting of a 1:1 mixture of donkey anti-goat and donkey anti-sheep IgG antibodies at 0.1 mg/mL, was deposited 5 mm downstream of each test line.

Assay execution involved applying 80 µL of recombinant biomarker standards, diluted across clinically relevant concentrations (0-1000 pM) in 1% BSA prepared in 1× PBS, directly onto the sample pads. After 3-minute incubation in the dark, 120 µL of running buffer was added to

initiate the run. Singleplex LFIAs were then incubated in the dark for an additional 20 minutes, allowing complete migration and analyte binding.

Fluorescence intensities were captured using the PROVIDS system. Dose-response curves were generated by plotting test-to-control intensity ratios (T/C) against known biomarker concentrations. Data were analyzed by fitting to a four-parameter logistic (4PL) regression model for accurate quantification of analytical performance parameters.

Triplex Quantitative LFIA of Human PR, ER, and HER2 Proteins

For full-strip triplex LFIA simultaneously targeting human PR, ER, and HER2 proteins, individual singleplex LFIA strips prepared as previously described were arranged in parallel with a 3 mm edge-to-edge spacing. Each strip interfaced with a shared 10 mm × 18 mm sample pad through standardized 2 mm overlaps, selected to ensure reproducible capillary flow while preventing lateral fluid crossover between adjacent nitrocellulose membranes.

Triplex assay execution involved applying 240 μL aliquots of recombinant biomarker mixtures, diluted in 1% BSA prepared in 1× PBS, onto the common sample pad. Following a 3-minute incubation period in the dark, 360 μL running buffer was immediately applied. The triplex LFIA strips were incubated in the dark for an additional 20 minutes to ensure complete analyte binding and fluid migration. Fluorescence imaging and quantification of PR, ER, and HER2 were performed using the PROVIDS system. Dose-response curves for each biomarker were established by plotting T/C ratios against their respective concentrations. Analytical performance was quantified by fitting these data to a 4PL regression model.

Evaluation of Cross-Reactivity and Specificity in Triplex LFIA

To evaluate the cross-reactivity and specificity of the triplex LFIA targeting PR, ER, and HER2 proteins, recombinant protein solutions were prepared individually at high, clinically relevant concentrations (1000 pM) for each biomarker, with the other two biomarkers set at 0 pM. This approach simulated critical edge-case scenarios to rigorously assess potential nonspecific interactions.

Fluorescence signals for PR, ER, and HER2 were simultaneously captured using the PROVIDS imaging system. Signal intensities at both targeted (spiked biomarker) and non-targeted (absent biomarker) test lines were quantitatively analyzed, and cross-reactivity ratios were calculated by comparing the intensity at non-target lines relative to the corresponding targeted test line intensity. The mean cross-reactivity ratios along with standard deviations were computed. Statistical consistency between singleplex and triplex formats was assessed using paired Student's t-tests, with statistical significance defined at $p > 0.05$.

Additionally, a 4PL regression model was applied to determine the baseline fluorescence signal (minimum asymptote, d) in the absence of target biomarkers, providing further validation of assay specificity. Confidence intervals (95% CI) were derived from the regression analysis to confirm the stability and precision of the specificity measurements.

Comparative Analysis of Triplex LFIA with ELISA

To establish clinically relevant subtype-specific cutoffs for the triplex LFIA, a total of thirty recombinant protein samples per biomarker (PR, ER, HER2) were selected to represent a broad spectrum of physiologically and clinically relevant concentrations reflective of breast cancer molecular subtypes.

Human PR, ER, and HER2 ELISAs were performed in accordance with the protocols detailed in the respective DuoSet ELISA kit manuals (R&D Systems). Briefly, recombinant protein samples (100 µL per well) were incubated on ELISA plates pre-coated with capture antibodies for 2 hours at room temperature. Plates underwent three wash cycles with PBST (0.05% Tween-20 in PBS), followed by a subsequent incubation with biotinylated detection antibodies for another 2 hours. Post-washing, streptavidin–HRP (100 µL per well) was added for 20 minutes, washed again, and then incubated with substrate solution. Optical density (OD) measurements were recorded at 450 nm using a SpectraMax MiniMax 300 Imaging Cytometre (Molecular Devices).

In parallel, identical recombinant samples were evaluated using the triplex LFIA, with fluorescence intensities captured for PR, ER, and HER2 using the PROVIDS system. Linear regression analyses were performed to evaluate the correlation between LFIA and ELISA measurements for each biomarker, using coefficients of determination (R^2) as quantitative indicators of agreement. Bland-Altman analyses were employed to assess systematic biases and calculate 95% limits of agreement between the LFIA and ELISA methods. The precision of the triplex LFIA was additionally quantified by calculating root mean square error (RMSE) values, providing an objective assessment of assay accuracy and variability. These comprehensive statistical analyses enabled the establishment of clinically relevant, subtype-specific cutoff values, aligning the LFIA detection capabilities with established diagnostic thresholds.

Validation of Triplex LFIA with Human Breast Cancer Tissue Lysates

Human Breast Cancer Tissue Lysates: Commercially sourced human breast cancer lysates were obtained from OriGene (CP565605 and CP537436), each supplied with vendor-annotated PR, ER, and HER2 molecular profiles (Supplementary Table S6-2). Lysates were stored at –80 °C and thawed on ice immediately prior to use. No additional pretreatment or matrix modification was performed to preserve the native proteomic composition.

ELISA Quantification: PR, ER, and HER2 concentrations in each lysate were quantified using DuoSet ELISA kits following the manufacturer's protocols. Lysates were diluted into the recommended dynamic range and dispensed to achieve an input of 2 µg total protein per well. Absorbance was measured at 450 nm with 570 nm reference subtraction, and blank-corrected values were fitted to a 4PL model. Analyte concentrations (pg/mL) were obtained by inverting the 4PL calibration curves. Measurements that fell below the assay lower limit of quantification (LLOQ) were reported as PR < 1.88 ng/mL and ER < 1.15 ng/mL and carried forward as LLOQ upper bounds for downstream comparative analyses.

Triplex LFIA Fabrication for Breast Cancer Tissue Lysates: Triplex LFIA strips were fabricated on HF135MC nitrocellulose membranes, selected for their balanced capillary wicking rate and

capacity to support complex lysate matrices. Spatially segregated PR, ER, and HER2 test lines were striped using biomarker-specific capture antibodies at 0.36 mg/mL to ensure sufficient binding capacity for crude lysate inputs. The donkey-IgG control line formulation remained unchanged relative to the recombinant-protein optimization workflow. Conjugate pad impregnation, membrane lamination, drying, and cutting were performed as described for the recombinant antigen assays.

Microfluidic Equalization Using a Passive Distributor: Singleplex test strips of each biomarker were assembled into a unified triplex cassette incorporating a passive microfluidic distributor upstream of the membrane. The network consists of trifurcating microchannels designed with matched hydraulic resistances to achieve equal volumetric delivery of the sample mixture to the PR, ER, and HER2 test strips. Channel geometries and mask-level dimensions are provided in Supplementary Figure 7. This equalization layer minimized lane-to-lane variability and ensured uniform sample exposure during lysate-based assays.

Triplex LFIA Quantification: Because crude lysates contain high protein loads and display elevated viscosity, all samples were diluted 1:5 using sample diluent buffer provided in DuoSet ELISA kits prior to LFIA analysis to promote uniform flow and prevent premature membrane fouling. For assay initiation, 240 µL of the diluted lysate was premixed with 300 µL of LFIA running buffer, resulting in a 540 µL sample-buffer mixture that was dispensed directly into the sample port of the triplex cassette. Fluorescence images were acquired using PROVIDS, and T/C ratios for each biomarker lane were extracted using the image-processing pipeline described in Supplementary Figure 4. Concentrations were determined by numerically inverting the biomarker-specific 4PL calibration functions derived from recombinant standards.

Normalization and Construction of Expression Matrices: To enable direct comparison between ELISA, which reports mass-based concentrations (ng/mL), and Triplex LFIA, which reports recombinant-equivalent concentrations (pM), all values were normalized within each biomarker independently. For biomarker B and sample S, normalized expression values were computed according to:

$$\text{Normalized}_{S,B} = \frac{\text{Concentration}_{S,B}}{\max\left(\text{Concentration}_{CP537436,B}, \text{Concentration}_{CP565605,B}\right)}$$

In this formulation, the higher-expressing lysate for each biomarker is assigned a normalized value of 1.00, and the lower-expressing lysate receives a fractional value (0–1). Prior to normalization, LFIA concentrations were converted to undiluted-equivalent pM values using the 1:5 dilution factor applied during sample preparation. ELISA values falling below assay LLOQ were normalized using their respective LLOQ upper bounds to maintain conservative estimates of inter-sample differences.

Design and Fabrication of the PROVIDS Reader

The PROVIDS reader housing was fabricated using a Raise3D Pro3 3D printer with black Polylactic Acid (PLA) filament. PLA was selected for its optical properties, as it effectively absorbs stray light, reducing interference during fluorescence measurements. Its mechanical

stability also ensures that the device maintains alignment and durability under repeated use in field environments. To optimize device assembly, key components such as the LFIA cartridge, UV-LED array mount, and camera enclosure were printed separately. These parts were assembled using precision alignment tools to achieve consistent placement of optical elements. The final housing design was iteratively refined to ensure compactness and to maintain precise alignment between the optical path and the test strip.

The optical components of the PROVIDS reader were selected to enhance fluorescence detection efficiency while ensuring safe and consistent illumination. Six low-power UV-A LEDs (DigiKey P6070T53040500) coaxially mounted on a custom PCB serve as the excitation source. The illumination assembly is fully enclosed within the reader housing, preventing exposure of users or bystanders to stray UV-A light. Fluorescence emission is collected through a 610/10 nm band-pass filter (Thorlabs), which isolates the narrow europium emission peak (~615 nm) and minimizes background interference. Images are recorded using a Raspberry Pi high-quality camera (Sony IMX477 sensor, 4056 × 3040 pixels) fitted with an adjustable lens to accommodate various LFIA configurations. The black PLA housing further stabilizes the optical path and suppresses ambient light, improving measurement precision.

LFIA Image-Processing Pipeline

The PROVIDS reader employs a Python-based software to automate image acquisition, processing, and biomarker quantification, ensuring robust and reproducible results across diverse experimental settings. While the *Main Manuscript* and *Supplementary Figure 4* outlines the general process, this section provides a comprehensive explanation of the algorithmic details, justifications for methodological choices, and steps to validate the pipeline's performance.

Image Capture and Region of Interest (ROI) Isolation: High-resolution images of the LFIA test strips are captured using a Raspberry Pi high-quality camera module, optimized for fluorescence detection through integrated controlled lighting. Consistent lighting and test strip location across all samples minimizes the impact of ambient interference, shadows, and uneven illumination, which could otherwise compromise data integrity. The LFIA Analyzer initiates automated cropping to isolate each Region of Interest (ROI), focusing on the fluorescence-active areas of each test strip. This targeted approach eliminates extraneous background regions, streamlining downstream analyses while maintaining computational efficiency.

Signal Extraction and Noise Reduction: Following ROI isolation, the cropped images are converted to grayscale and intensity profiles are extracted as a mean across the horizontal distance to capture fluorescence variations across the test strip. To improve signal clarity, the LFIA Analyzer applies a Gaussian filter ($\sigma = 5$) to the extracted signals. This filter effectively smooths the intensity profiles without distorting critical features such as line width, peak sharpness, and fluorescence height. Its design is particularly suited for handling fluorescence data, where maintaining the integrity of the signal is essential for accurate quantification. By mitigating high-intensity noise originating from the LFIA membrane or inconsistencies in sample flow, this step lays a solid foundation for reliable signal quantification.

Background Correction: The extracted image profiles include raw fluorescence data for both the test and control lines, as well as the surrounding background regions. Background intensity is calculated using the area between the detected test and control lines and subtracted from the raw signal to correct for nonspecific fluorescence. This background-subtracted profile improves quantification accuracy by removing any remaining noise from the smoothed intensity profiles.

Detection of Test and Control Lines: Using the refined intensity profiles, a function employed to identify the most prominent peaks within the test region. Peaks are assigned as test (It) or control (Ic) lines by comparison of their pixel position relative to the center of the ROI. The magnitude of these peaks is used to calculate the It/Ic ratio. This ratio-based quantification approach accounts for variability in strip-to-strip fluorescence intensity and ensures robust performance across a wide dynamic range.

Quantification of Biomarker Levels and Subtype Classification: The software quantifies biomarker concentrations by leveraging the test-to-control intensity ratio (It/Ic), which directly correlates with analyte concentration. Calculated It/Ic ratios are then related to 4PL dose-response curve equation parameters (Table S1) for each biomarker to quantify PR, ER, and HER2 concentration of the multiplexed test strips. These estimated concentrations are compared to the subtype specific cutoffs summarized in Table S3, to classify samples within the corresponding breast cancer subtype.

Visualization and Quality Control: The LFIA Analyzer generates visual outputs that overlay detected test and control lines on the original images, accompanied by annotations of peak positions and fluorescence intensity. Additionally, smoothed intensity profiles with background corrections are plotted to highlight the results of each processing step. These visual aids provide transparency and enable users to validate the accuracy of the automated pipeline. Quality control measures embedded within the algorithm flag discrepancies, such as missing lines or irregular profiles, prompting manual review when necessary.

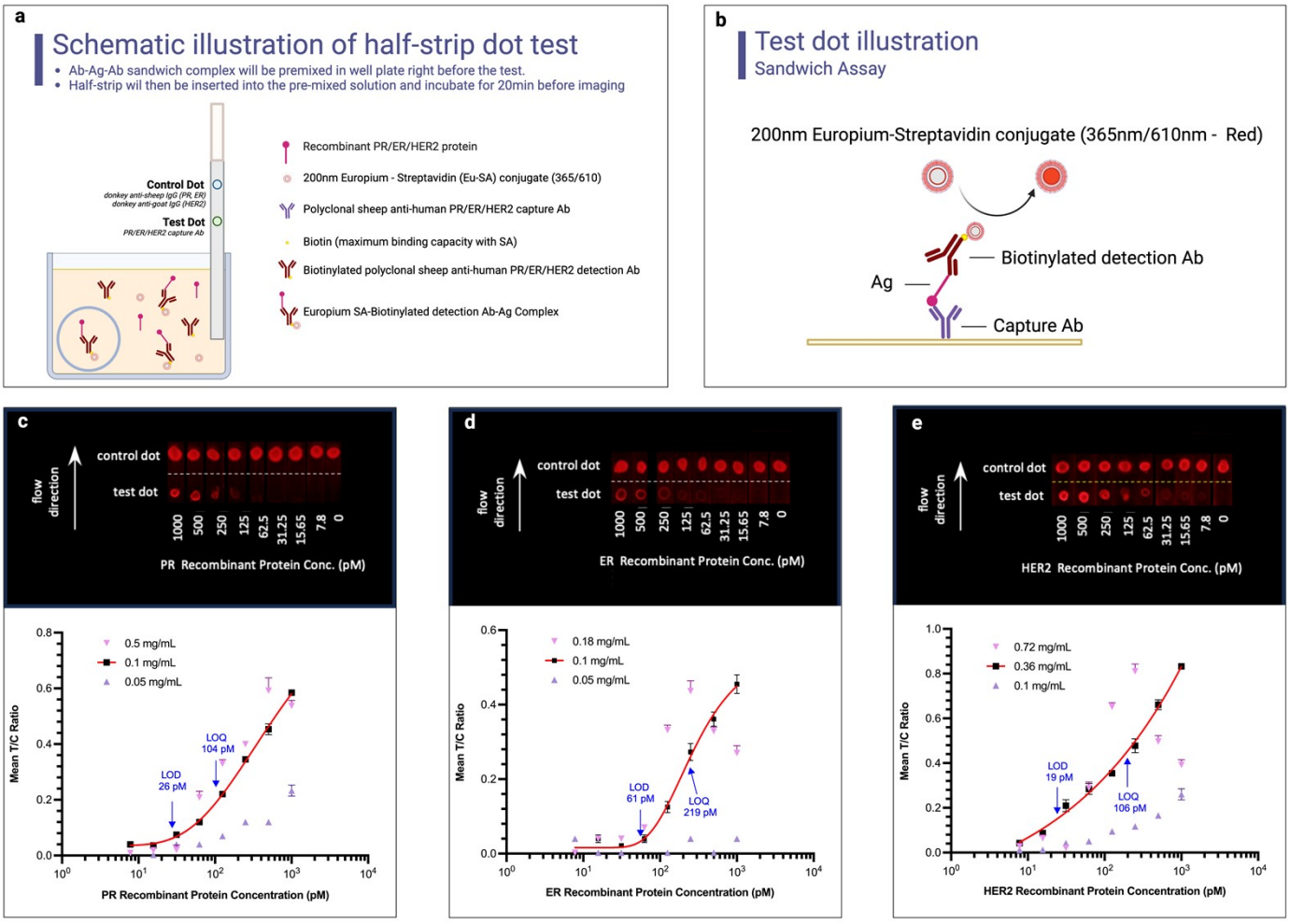

Supplementary Fig. 1: Optimization Secondary IgG Antibody Concentration of Singleplex LFIA

a, Schematic illustration of individual LFIA strips compromising human total PR/ER/HER2 capture antibody test dot and a donkey IgG control dot. **b,** Schematic illustration of the sandwich architecture of reagents at test dot. **c,** PROVIDS built-in code processed images and generated dose-dependent fluorescence intensities mean T/C ratio curve of human total PR LFIAs constitute of 0.5/0.1/0.05 mg/mL of capture antibody at capture site. Inset: fluorescence images of human total PR LFIAs constitute of 0.1 mg/mL of capture antibody at capture site. **d,** PROVIDS built-in code processed images and generated dose-dependent fluorescence intensities mean T/C ratio curve of human total ER LFIAs constitute of 0.18/0.1/0.05 mg/mL of capture antibody at capture site. Inset: fluorescence images of human total ER LFIAs constitute of 0.1 mg/mL of capture antibody at capture site. **e,** PROVIDS built-in code processed images and generated dose-dependent fluorescence intensities mean T/C ratio curve of human total HER2 LFIAs constitute of 0.72/0.36/0.1 mg/mL of capture antibody at capture site. Inset: fluorescence images of human total HER2 LFIAs constitute of 0.36 mg/mL of capture antibody at capture site. Data are mean ± s.d.; $n = 3$ repeated tests. Schematics were created with BioRender.com.

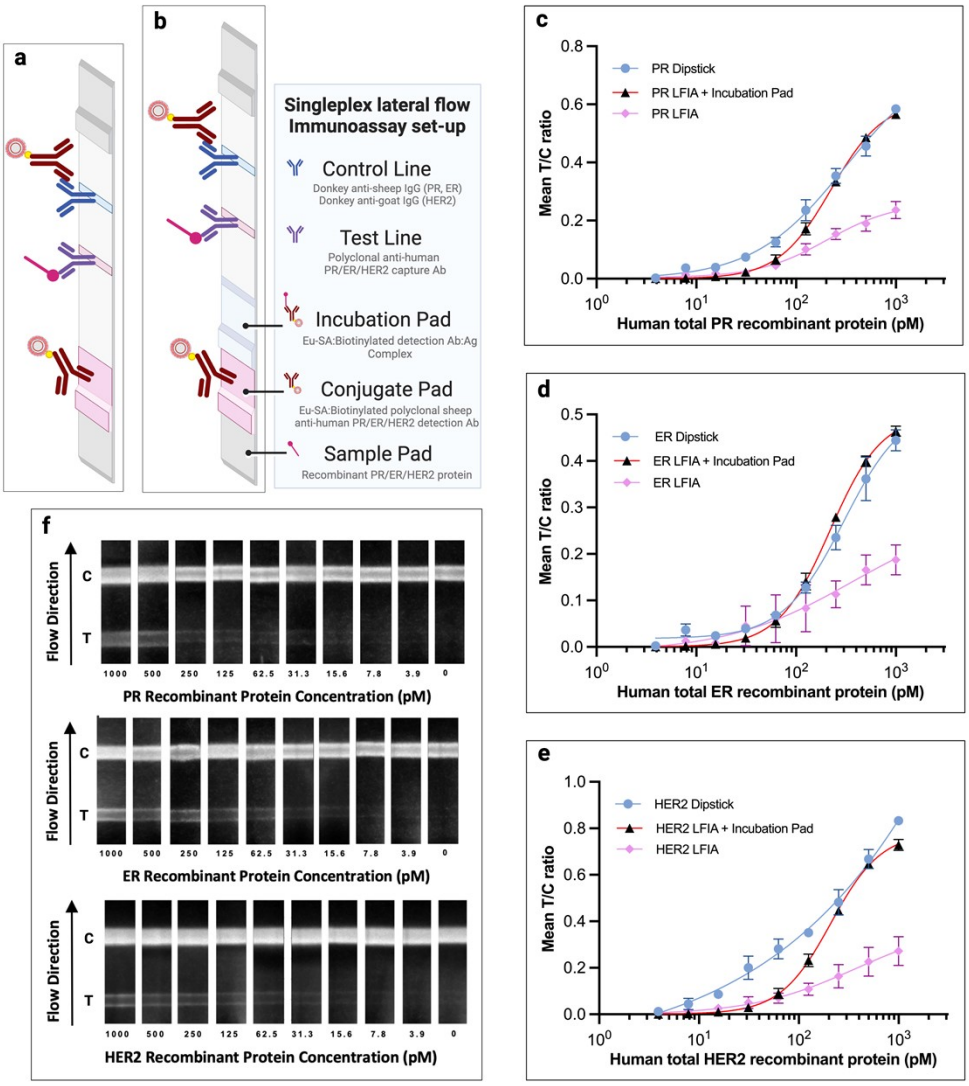

Supplementary Fig. 2: Optimization Singleplex LFIA Architect with Enhanced Fluorescence Outcomes

a, Schematic illustration of a conventional singleplex sandwich LFIA compromising an absorption pad, a human total PR/ER/HER2 capture antibody test line, and a donkey IgG control line, an [Eu-SA:Biotinylated detection antibody complex] overspread conjugation pad, and a sample pad. **b,** Schematic illustration of an optimized singleplex sandwich LFIA compromising an absorption pad, a human total PR/ER/HER2 capture antibody test line, and a donkey IgG control line, an [Eu-SA:Biotinylated detection antibody complex] overspread conjugation pad, an incubation pad for enhanced assay reaction, and a sample pad for analyte and buffer addition. **c,** Dose-dependent fluorescence intensities mean T/C ratio curves of singleplex human total PR LFIA dipsticks; singlplex LFIAs with conventional architect; and singleplex LFIAs with optimized architect in assembly. **d,** Dose-dependent fluorescence intensities mean T/C ratio curves of singleplex human total PR LFIA dipsticks; singleplex LFIAs with conventional

architect; and singleplex LFIAs with optimized architect in assembly. **e,** Dose-dependent fluorescence intensities mean T/C ratio curves of singleplex human total ER LFIA dipsticks; singleplex LFIAs with conventional architect; and singleplex LFIAs with optimized architect in assembly. **f,** Dose-dependent fluorescence intensities mean T/C ratio curves of singleplex human total HER2 LFIA dipsticks; singleplex LFIAs with conventional architect; and singleplex LFIAs with optimized architect in assembly. **g,** Fluorescence images of optimized human total PR/ER/HER2 singleplex LFIAs. Data are mean ± s.d.; $n = 4$ repeated tests. Schematics were created with BioRender.com.

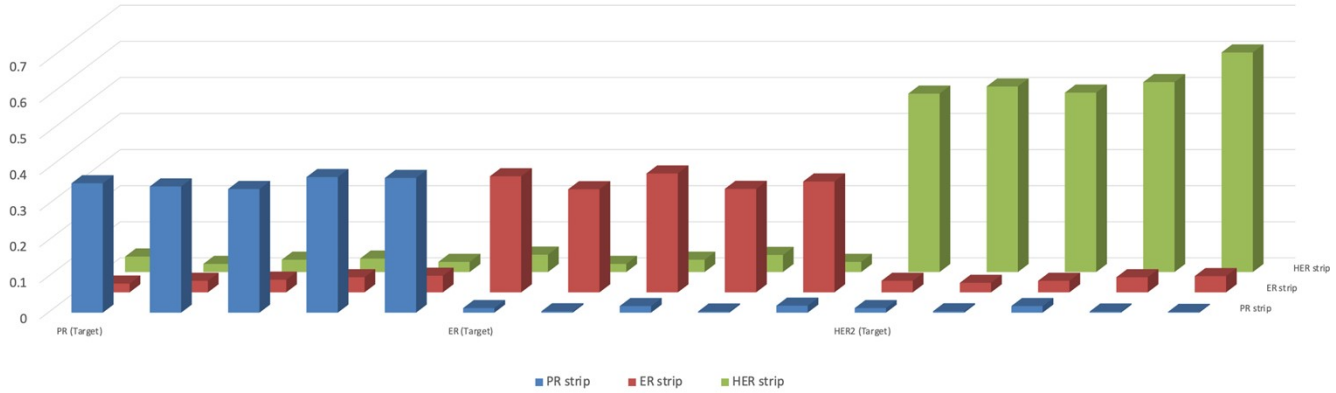

Supplementary Fig. 3: Cross-reactivity analysis of the triplex LFIA with PR, ER, and HER2 spiking conditions

Bar plot demonstrating the fluorescence mean T/C ratios for PR, ER, and HER2 spiked at 1000 pM, evaluated across PR, ER, and HER2 test lines to assess cross-reactivity. PR-specific signals (blue bars), ER-specific signals (red bars), and HER2-specific signals (green bars) are shown for each spiking condition. Each target exhibits robust signals on its corresponding test line, with minimal cross-reactivity observed on non-target test lines. Data represent the mean fluorescence T/C ratios, highlighting the specificity of the triplex LFIA architecture. Data are mean ± s.d.; n = 5 repeated tests.

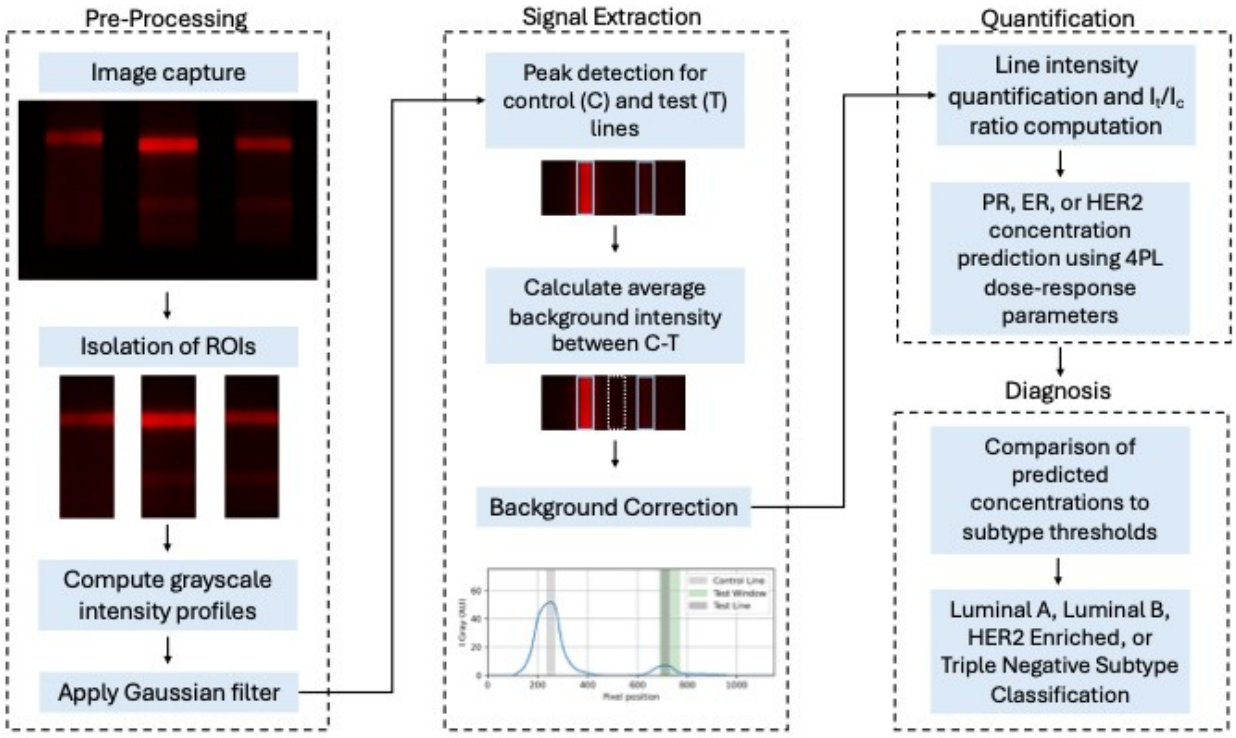

Supplementary Fig. 4: PROVIDS In-Built LFIA Image Processing Pipeline

This figure illustrates the PROVIDS in-built LFIA image processing pipeline, which automates biomarker detection and quantification. After capturing high-resolution LFIA images under controlled lighting, the pipeline isolates the Region of Interest (ROI) containing the test (T) and control (C) lines. Preprocessing includes denoising with a Gaussian filter and peak detection algorithms to distinguish line fluorescence from the background. The software detects line positions based on fluorescence intensity and geometric features, followed by generating horizontal intensity profiles. Background subtraction is performed to correct nonspecific signals, and the test-to-control intensity ratio (It/Ic) is calculated. This ratio is mapped against a calibration curve to determine the concentration of the investigated biomarker and compared with subtype-specific cutoffs to classify the samples, with results displayed in real time.

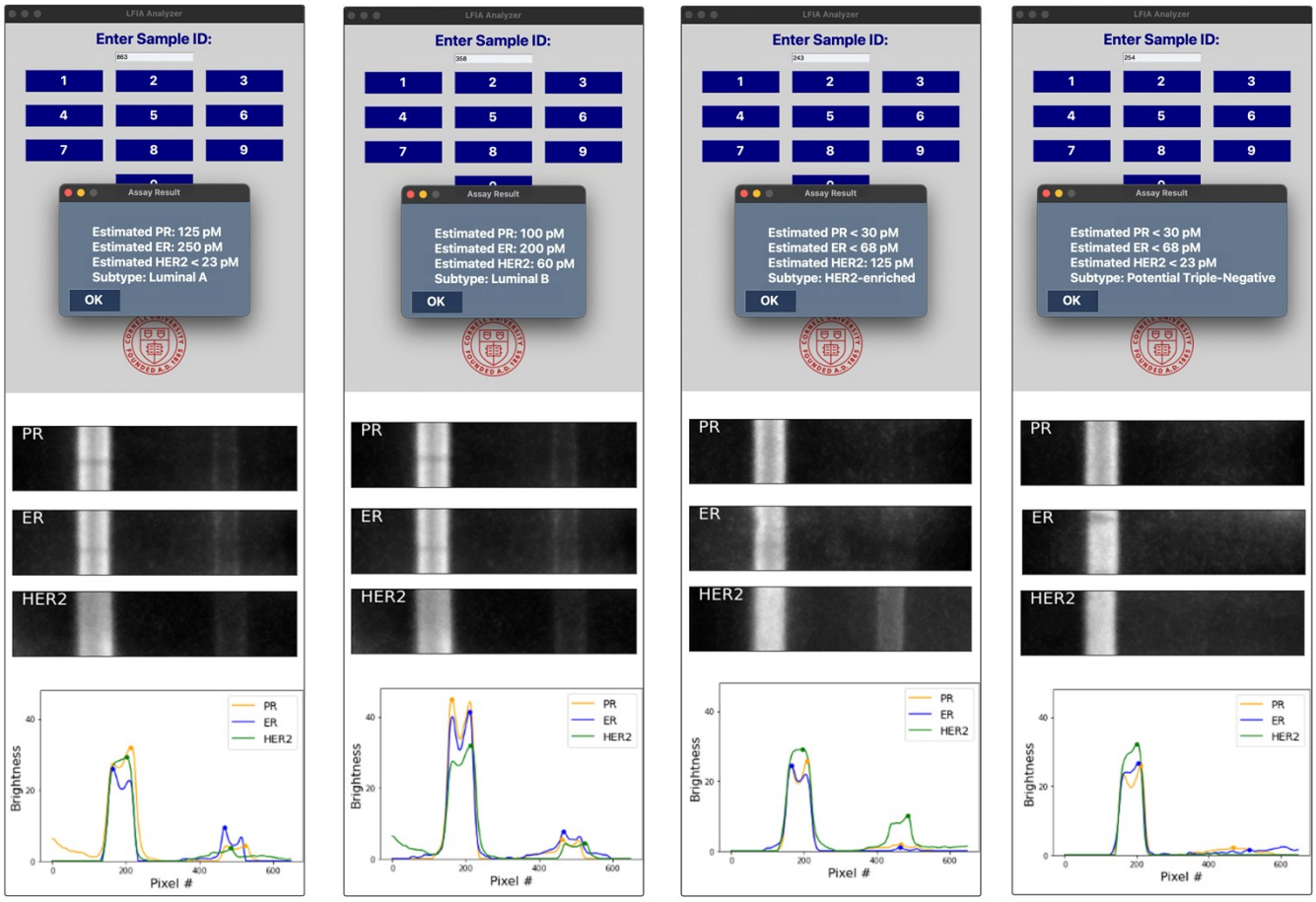

Supplementary Fig. 5: Representative Breast Cancer Subtype Profiles and User Report Formats

This figure presents grayscale images and intensity profiles for breast cancer subtype-specific representative samples. Luminal A (PR high, ER positive, HER2 negative) shows strong PR and ER signals, while Luminal B (PR positive, ER positive, HER2 negative) displays moderate fluorescence for PR and ER. HER2-enriched subtypes (PR low, ER low, HER2 high) exhibit a dominant HER2 signal, and TNBC (PR negative, ER negative, HER2 negative) demonstrates minimal fluorescence across all lines. The user interface reports quantitative biomarker concentrations or cutoff-based labels, such as "< [cutoff concentration]," and assigns subtype classifications based on clinical thresholds. Visual outputs include numerical results for rapid interpretation in clinical settings, grayscale images, fluorescence intensity profiles.

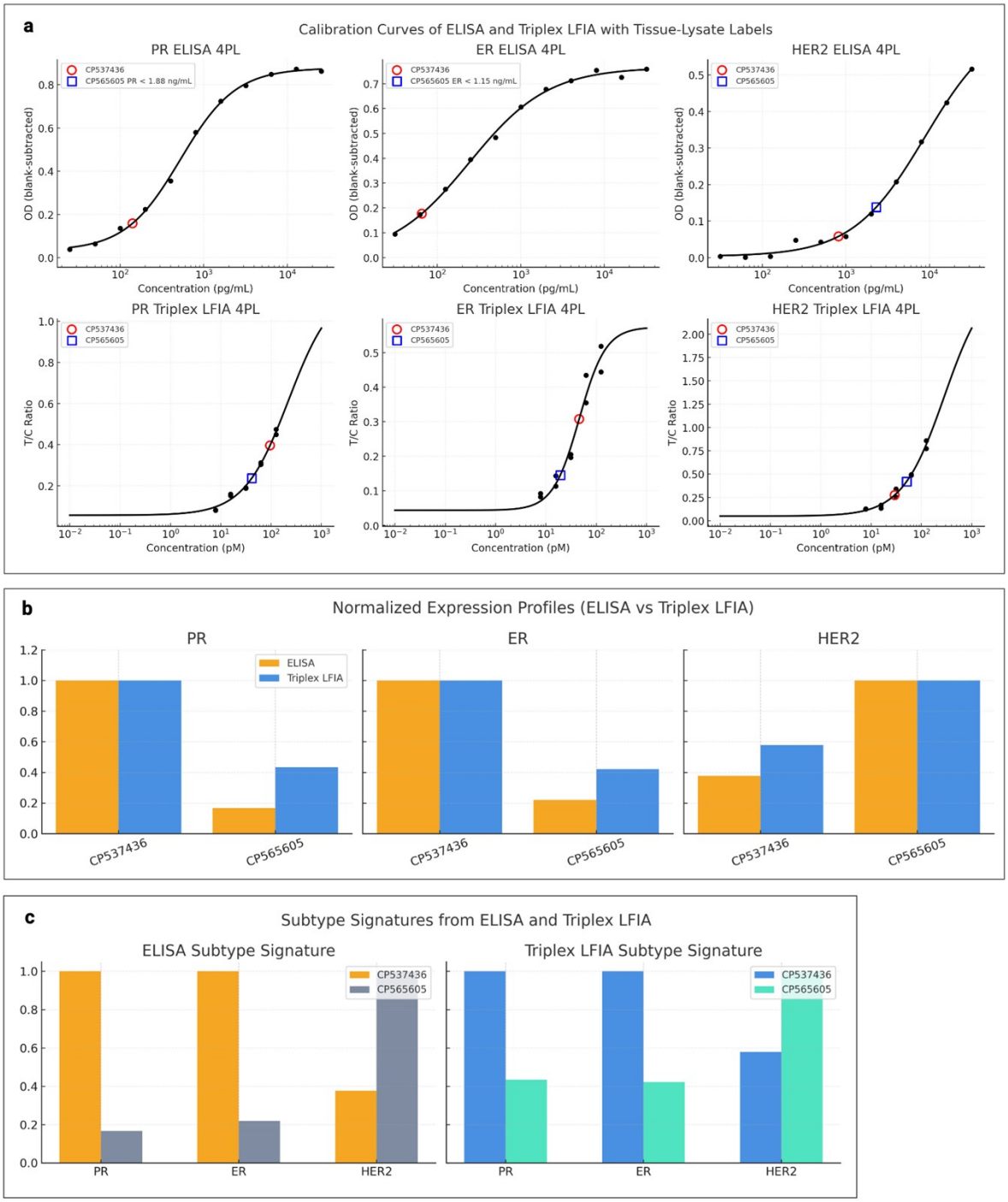

Supplementary Fig. 6: Quantitative Validation of Triplex LFIA Performance in Human Breast Cancer Tissue Lysates

a, *Calibration curves for PR, ER, and HER2 ELISAs and Triplex LFIA with tissue-lysate positions.* ELISA panels (top row) show four-parameter logistic (4PL) calibration curves generated from recombinant standards (n = 2 technical replicates per concentration), plotted as

blank-subtracted OD versus working concentration in the assay well (pg/mL). Tissue-lysate points represent the analyte concentrations present in the ELISA wells after loading 2 µg of total lysate protein per well (n = 3 technical replicates). For CP537436 (ER^+/PR^+), the corresponding concentrations measured in the ELISA wells were 140.8 pg/mL PR**,** 65.46 pg/mL ER, and 816.22 pg/mL HER2. For CP565605 ($HER2^+$), PR and ER signals at the same protein input were below the ELISA lower limit of quantification (reported as PR < 1.88 ng/mL and ER < 1.15 ng/mL) and therefore are listed in the legend rather than plotted. HER2 for CP565605 (2306.26 pg/mL) was within the ELISA calibrated range and is shown as a blue open square. Triplex LFIA panels (bottom row) show 4PL calibration curves plotting T/C Ratio versus recombinant concentration (pM). Tissue lysate T/C ratios were converted to recombinant-equivalent concentrations using the LFIA calibration curves and corrected for the 1:5 sample pre-dilution, yielding diluted-equivalent concentrations of 95.3, 45.8, and 29.4 pM for CP537436 and 41.3, 19.3, and 50.8 pM for CP565605 in the PR, ER, and HER2 channels, respectively. All LFIA tissue-lysate points fall within the calibrated LFIA dynamic range. **b,** *Normalized PR, ER, and HER2 expression measured by ELISA and Triplex LFIA in breast cancer tissue lysates.* For each biomarker, ELISA (ng/mL) and Triplex LFIA (recombinant-equivalent pM) concentrations were independently normalized to the maximum value across the two lysates to enable unit-independent comparison. CP537436 (ER^+/PR^+) exhibits high PR and ER expression and moderate HER2 expression by both ELISA and LFIA. CP565605 ($HER2^+$) shows low PR/ER expression and high HER2 expression across both platforms. Despite different calibration chemistries (mass-based ng/mL for ELISA and recombinant-equivalent pM for LFIA), the normalized expression profiles preserve the same relative biomarker hierarchy for each sample, demonstrating that Triplex LFIA reproduces the overall expression pattern observed by ELISA in real tissue lysates. **c,** *Subtype-defining biomarker signatures derived from ELISA and Triplex LFIA.* Subtype signatures were generated by plotting normalized PR, ER, and HER2 expression for each sample across the three biomarkers. Both platforms identify CP537436 (ER^+/PR^+) as PR-high / ER-high / HER2-low and CP565605 ($HER2^+$) as PR-low / ER-low / HER2-high. Preservation of this subtype pattern across ELISA and Triplex LFIA demonstrates that the LFIA not only quantifies each biomarker but also accurately reproduces clinically meaningful expression hierarchies, supporting its potential for translational subtype determination using crude tissue lysates.

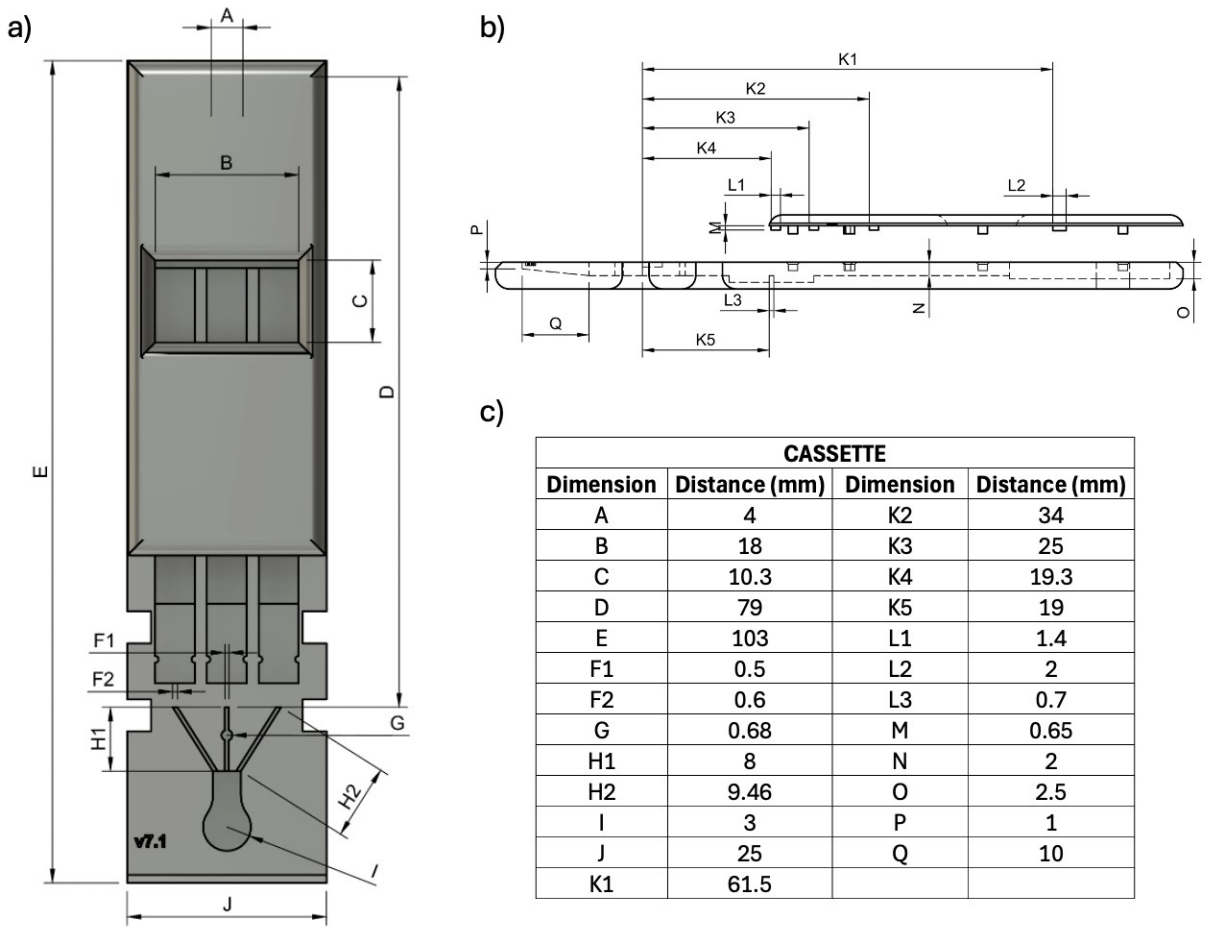

c)

CASSETTE			
Dimension	Distance (mm)	Dimension	Distance (mm)
A	4	K2	34
B	18	K3	25
C	10.3	K4	19.3
D	79	K5	19
E	103	L1	1.4
F1	0.5	L2	2
F2	0.6	L3	0.7
G	0.68	M	0.65
H1	8	N	2
H2	9.46	O	2.5
I	3	P	1
J	25	Q	10
K1	61.5		

Supplementary Fig. 7: Computer-aided design (CAD) of the Triplex LFIA Cassette Incorporating the Passive Microfluidic Distributor for Sample Division

a, Top-view rendering showing the overall cassette geometry and the layout of the trifurcating microchannels upstream of the nitrocellulose membrane. **b,** Side-view schematic illustrating the cassette architecture, channel thickness, and alignment of the membrane and housing components. **c,** Table summarizing all annotated dimensions (mm) corresponding to the labeled microfluidic and structural design features.

Table S1. Parameters for Sigmoidal Curve Fits of PR, ER, and HER2 in Singleplex and Triplex LFIA

Biomarkers	Parameter	Coefficient (Singleplex)	SE (Singleplex)	95% CI for LogIC50 (Singleplex)	Coefficient (Triplex)	SE (Triplex)	95% CI for LogIC50 (Triplex)
PR	d	-0.001541	0.00087	-0.02293 to 0.01436	-0.01926	0.00125	-0.1074 to 0.009142
	a	0.6292	0.0133	0.5454 to 0.8087	0.5395	0.0154	0.3929 to 0.6861
	c	2.497	0.0485	2.362 to 2.760	2.588	0.0634	2.257 to 2.819
	b	0.9428	0.0126	0.7321 to 1.157	0.7322	0.0187	0.2869 to 1.104
ER	d	0.0139	0.0021	-0.0004386 to 0.02618	0.01717	0.0031	0.004127 to 0.02939
	a	0.4629	0.0342	0.4074 to 0.5770	0.3043	0.0451	0.2723 to 0.3600
	c	2.482	0.0453	2.384 to 2.663	2.353	0.0532	2.268 to 2.481
	b	1.452	0.178	1.078 to 1.890	2.212	0.23	1.484 to 3.388
HER2	d	-0.07721	0.0071	-0.3145 to 0.007079	-0.06876	0.0059	-0.1864 to 0.01635
	a	1.609	0.0325	1.5453 to 1.6727	3.913	0.0468	3.8213 to 4.0047
	c	3.206	0.0871	3.0353 to 3.3767	4.945	0.0946	4.7596 to 5.1304
	b	0.4819	0.0483	0.3872 to 0.5766	0.3862	0.0562	0.2760 to 0.4964

This table provides the parameters and corresponding standard errors (SE) obtained from sigmoidal curve fits for PR, ER, and HER2 biomarkers in both singleplex and triplex LFIA formats. The 4PL regression equation used is Y = d + (a - d)/(1 + (X/c)^b), where *a* represents the baseline response at low analyte concentrations, *d* indicates the maximum response at high concentrations, *c* (LogIC50) is the concentration at which the response is halfway between *a* and *d*, and *b* reflects the steepness of the curve (Hill slope). The R^2 values, which indicate the goodness of fit for the regression model, are 0.9886 for PR, 0.9755 for ER, and 0.9737 for HER2 in the singleplex format, and 0.9624 for PR, 0.9429 for ER, and 0.9632 for HER2 in the triplex format.

Spiked Biomarker (1000 pM)	Test Line	Mean T/C Ratio (%)	Standard Deviation (%)
PR	PR	35.98	± 1.52
	ER	3.41	± 0.81
	HER2	3.55	± 0.72
ER	PR	1.44	± 0.61
	ER	31.14	± 1.75
	HER2	3.31	± 0.61
HER2	PR	1.21	± 0.54
	ER	2.76	± 0.78
	HER2	50.96	± 2.13

Table S2. Cross-Reactivity Analysis of PR, ER, and HER2 in Triplex LFIA

This table summarizes the mean T/C ratios (%) ± SD for PR, ER, and HER2 biomarkers spiked at 1000 pM, measured across target and non-target test lines to evaluate assay specificity. Data include normalized fluorescence signals averaged across replicates, with standard deviations representing variability. Each row presents target-specific signals and cross-reactivity levels to assess the performance of the triplex LFIA in minimizing nonspecific interactions.

Subtype	PR Cutoff (pM)	ER Cutoff (pM)	HER2 Cutoff (pM)
Luminal A	PR > 100 pM	ER > 100 pM	HER2 < 23 pM
Luminal B	PR: 50–150 pM	ER: 68–200 pM	HER2: 23–60 pM
HER2-enriched	PR < 30 pM	ER < 68 pM	HER2 > 60 pM
Triple-Negative (TNBC)	PR < 30 pM	ER < 68 pM	HER2 < 23 pM

Tabel S3. Subtype-Specific Biomarker Cutoffs for Triplex LFIA

This table defines the refined biomarker cutoffs for breast cancer subtype classification using the triplex LFIA system. Derived from comparative analysis with ELISA, the cutoffs reflect triplex LFIA's detection capabilities while maintaining clinical relevance. Subtypes are categorized based on PR, ER, and HER2 expression profiles, ensuring accurate classification for Luminal A, Luminal B, HER2-enriched, and TNBC.

Component	Unit Price	Usage per Triplex Test	Cost per Test
Europium–streptavidin nanoparticles (Abcam ab270228, 0.5% solids)	$375/mL	0.04 µL stock	**$0.02**
Detection antibodies (PR, ER, HER2; R&D Systems DuoSet)	$475 per kit	~0.07–0.12 µg total	**$0.18**
Capture antibodies (PR, ER, HER2; R&D Systems DuoSet)	Included above	~0.10–0.36 µg	**$0.06**
Control-line donkey IgG (Bio-Techne BAF109 & BAF016)	$129/100 µg	0.10 µg	**$0.13**
Nitrocellulose membrane (Cytiva FF170/FF180)	$10 per sheet	~1.5 cm^2/test	**$0.03**
Sample, conjugate, incubation, absorbent pads	$10–$15 per sheet	per-test fraction	**$0.03**
Running buffer/conjugation buffer/blocking buffer	<$0.01 each	—	**$0.01**
Total Cost per Triplex LFIA	—	—	**$0.30–$0.35**

Tabel S4. Raw Material Cost Decomposition for the Triplex LFIA

This table defines the Individual cost contributions from europium–streptavidin nanoparticles, detection and capture antibodies, control-line antibodies, nitrocellulose membranes, sample/conjugate/incubation/absorbent pads, and buffers were calculated using vendor pricing and experimentally determined reagent volumes. The resulting per-test cost of $0.30–$0.35 is comparable to or below commercially reported multiplex AuNP-based LFIA formats.

Table S5. Vendor-provided molecular characterization of OriGene breast cancer lysates used for real-sample validation

Lysate ID	Vendor Subtype Annotation	ER Status (Vendor)	PR Status (Vendor)	HER2 Status (Vendor)	Reported Vendor Characterization Method	Biological Matrix	Intended Use (Vendor)	Expected Molecular Phenotype
CP565605 ($HER2^+$)	HER2-overexpressing breast carcinoma	Negative / low	Negative / low	Positive (HER2-high)	Internal immunoassay QC (IHC / antibody profiling)	Human breast carcinoma lysate	Positive control lysate for HER2-high breast cancer	**HER2-enriched** ($ER-$ / $PR-$ / $HER2^+$)
CP537436 (ER^+/PR^+)	Hormone receptor–positive breast carcinoma	Positive	Positive	Negative–intermediate (HER2-low)	Internal immunoassay QC (IHC / antibody profiling)	Human breast carcinoma lysate	Positive control lysate for ER+/PR+ breast cancer	**Luminal B–like** (ER^+ / PR^+/ HER2-low)

This table summarizes the receptor-status annotations supplied by OriGene for the two human breast cancer lysates evaluated in this study. CP565605 is characterized as a HER2-overexpressing carcinoma with low/negative ER and PR expression, while CP537436 is annotated as a hormone receptor–positive carcinoma exhibiting ER^+/PR^+ profiles with low HER2 expression. Vendor characterization was performed through OriGene's internal immunoassay quality control pipeline (e.g., IHC or antibody-profiling methods). These annotations were used as independent reference phenotypes for confirming subtype agreement in *Supplementary Figure 6*.